

Research Article

Application of Photoacoustic Methods and Confocal Microscopy for Monitoring of Therapeutic Response in Plaque Psoriasis

Katharina Ossadnik^a Sandra Philipp^a Wolfgang Bost^b Marc Fournelle^b
Heike Richter^a Jürgen Lademann^a^aCharité – Universitätsmedizin Berlin, Corporate Member of Freie Universität Berlin, Humboldt-Universität zu Berlin, and Berlin Institute of Health, Department of Dermatology, Venerology and Allergology, Berlin, Germany;^bFraunhofer Institut für Biomedizinische Technik IBMT, St. Ingbert, Germany**Keywords**

Photoacoustic techniques · Confocal laser scanning microscopy · Psoriasis · Capillaries

Abstract

Psoriasis is prone to relapses and requires long-term therapy that may induce a range of adverse effects; therefore, an efficient and early detection of relapses is desirable. In this study, photoacoustic imaging and confocal laser scanning microscopic (CLSM) methods were investigated for their suitability in psoriasis follow-up examinations. Using a high-resolution photoacoustic system, the vascular structures of 11 psoriatic patients and 6 healthy volunteers were investigated. No differences were detected with respect to the average vessel diameter and vasculature per unit volume in the tissue of healthy volunteers and non-lesional and lesional skin areas of psoriatic patients. By means of CLSM, the diameters of the dermal papillae of 6 volunteers and 6 psoriatic patients were determined. The diameters of the dermal papillae of the healthy volunteers (0.074 ± 0.006 mm) revealed no significant difference when compared to non-lesional skin areas of psoriatic patients (0.079 ± 0.005 mm). The results obtained for the lesions in psoriatic patients showed a significant difference (Wilcoxon test, $p = 0.028$) between the diameters of the dermal papillae of the lesional skin areas

(0.114 ± 0.012 mm) and the non-lesional skin areas (0.079 ± 0.005 mm). Thus, CLSM can be applied for monitoring psoriasis follow-up examinations.

© 2018 S. Karger AG, Basel

Introduction

With prevalence rates in adults reported to be between 0.51 and 11.43%, psoriasis is one of the most frequent inflammatory skin diseases [1]. In Germany alone, about 2 million people are affected by this condition. For the affected subjects, psoriasis often entails a considerable stigma as well as restrictions with regard to their quality of life and their physical and mental health [2, 3]. The annual health care costs are substantial. In a disease-cost study conducted in Germany, it was shown that the annual total expenditure per patient amounts to approximately EUR 3,000 and even to approximately EUR 5,000, if the patient additionally undergoes systemic therapy [4]. In a clinical study, it was demonstrated that the restrictions to the physical and mental abilities of psoriatic patients are comparable to the physical and mental abilities of patients suffering from cancer, diabetes, cardiac diseases, hypertension, arthritis, or depression [5]. The pathogenesis of this disease, although not yet completely understood, is multifactorial,

involving both genetic and environmental factors. Psoriasis is currently considered to be a T-cell mediated inflammatory reaction [6, 7]. The activation of T-cells stimulates the formation of mediators which, in turn, bring about the typical structural vascular and epidermal changes in psoriatic skin. Previous investigations elucidated the impact of the changes in the vascular architecture for the pathogenesis of psoriasis. Electron microscopic investigations predominantly revealed changes in the capillary loops inside the dermal papillae which, contrary to the capillary loops of healthy skin, are multiply twisted and elongated and lose their typical hairpin shape [8, 9].

Beside basic therapy, psoriasis treatment is based on 3 pillars, namely topical, photo, and systemic therapy. In daily clinical practice, biomarkers for standardized psoriasis monitoring are not yet available. For the assessment of the severity of the disease and the therapeutic success, several scoring systems are used. In Europe, primarily the Psoriasis Area Severity Index and, for the assessment of the disease-related quality of life, the Dermatology Life Quality Index have become established [10]. Beyond a reduction of the skin symptoms and monitoring of the disease progression, an efficient psoriasis therapy is aimed at minimizing the side effects and obtaining a long-term remission [11]. Due to the chronically recurring progression, often requiring long-term therapy, adverse drug effects, and high expenses of an immunosuppressive therapy, it would be preferable to know whether only superficial lesions are cured by this therapy. If so, sub-clinical changes will remain and promote the development of recurrences. An efficient early detection of relapses and also the possibility of reducing or interrupting the systemic therapy in the case of successful treatment would be of great advantage.

Using laser scanning microscopy, Archid et al. [12] found widened diameters of both capillaries and papillae in psoriatic versus healthy skin, and a correlation between clinical alleviation and normalization of the skin structure. Wolberink et al. [13] showed a high agreement between confocal laser scanning microscopy (CLSM) and histological investigations using light microscopy when detecting the structural changes as well as a clear correlation between clinical alleviation of psoriasis and the detection of the normalization of the structural changes by laser scanning microscopy and light microscopy [13].

Laser scanning microscopy is an already established, non-invasive in vivo imaging method which might provide an option to assess the therapy success and define if a therapy must be continued until normalization of the structural skin changes is reached. However, examinations by laser scanning microscopy require highly spe-

cialized staff, sophisticated microscopy systems, and are rather time consuming.

Alternatively to laser scanning microscopy, photoacoustic imaging could be applied. Photoacoustic imaging is an innovative, non-invasive procedure, which has become increasingly popular in recent years. It is based on the generation of broadband acoustic transients as a result of localized optical absorption of short time laser pulses, thus joining the advantages of optical and acoustic methods. Compared to the purely optical procedures, photoacoustic imaging is characterized by an increased penetration depth, and compared to purely acoustic methods, by providing higher contrast between different types of tissue. All this indicates that photoacoustic imaging is promising for future establishment in clinical use [14, 15]. The added diagnostic value of photoacoustics has been documented in many publications. In first investigations, for example, the application potential of this novel technique in breast cancer diagnostics was shown [16, 17]. Preclinical investigations on skin could reveal its possible importance for dermatology, specifically for staging of melanoma, for example, prior to surgery [18] or for determining the depth of thermal burns [19]. Favazza et al. [20, 21] could demonstrate that photoacoustic imaging is specifically suitable for representing the vascularization of the skin.

The present study was aimed to investigate photoacoustic imaging and CLSM for their applicability in follow-up examinations of psoriasis.

Material and Methods

Photoacoustic Imaging System "SKINSPECTION"

For the measurements, the Fraunhofer Institut für Biomedizinische Technik IBMT (St. Ingbert, Germany) provided us with a system that had been developed in collaboration with the company Kibero (Kibero GmbH, Saarbrücken, Germany) within the European research project "SKINSPECTION." This system integrates a single-element focused ultrasonic transducer of 35 MHz center frequency for detecting of acoustic waves. It consists of an acoustic lens (curved active area) with a curvature radius of 5.5 mm and an active area of 5 mm in diameter. The bandwidth of the transducer was measured to be 100% and the extent of the -6 db focal zone was 100 μ m in lateral and 2.4 mm in axial direction. For digitization of the optical generated ultrasonic signals and controlling the linear stages that are required for moving the ultrasonic transducer mechanically within a 2-dimensional grid, a single-channel ultrasonic electronics including a PC has been developed.

A frequency doubled Nd:YAG laser system (FDSS 532-150, CryLas GmbH, Germany), generating an optical light pulse of 532 nm, has been used for the photoacoustic signal generation. The pulse energy can be defined by the user up to maximum values of 37 μ J with a repetition rate of 1 kHz. The pulse length of 1.5 ns ensures that high frequency ultrasonic signals are generated in order

to match the frequency of the used transducer. For targeted light delivery, the light is coupled into a custom-made fiber bundle whose geometry strongly defines the size and the pattern of the irradiated area on the skin surface. In addition, the system is equipped with a PC, a hand-held sensor head accommodating both the transducer and the motorized positioning unit, and a tailor-made software for visualizing the acquired data.

In a standard ultrasonic procedure, an acoustic wave is transmitted into the target tissue and the amplitude of reflected signal portion is measured. However, in the photoacoustic imaging mode, the source of the acoustic waves is the tissue itself. Photoacoustic signals are generated based on the thermoelastic effect describing the absorption of pulsed electromagnetic radiation on tissue structures with high optical absorption coefficients and the transformation into heat and pressure [22–24]. If this effect is subject to thermal and acoustic confinement, the thermal increase leads to a volume expansion of the tissue. The resulting local pressure propagates as acoustic waves, which can be detected by appropriate sensors and converted into an electrical signal [25]. The penetration depth of the light into the tissue and the contrast of photoacoustic imaging are predominantly influenced by the optical properties of the tissue to be investigated and the wavelength of the optical light pulse selected for imaging. The absorption coefficient of melanin, oxy-(HbO₂) and deoxyhemoglobin (HHb) decreases with increasing wavelength in the near infrared spectral region, whereas the absorption of water and fat is enhancing [26–28]. The wavelength range from 600 to 1,100 nm is called the optical window. In this optical window, structures at increased depths can well be investigated as the overall tissue absorption coefficient decreases to a minimum and the tissue scattering is reduced in this range [24, 27, 29]. In contrast, light in the range around 500 nm is already absorbed in the uppermost dermal layers due to the extremely high absorption of hemoglobin, which on the other hand leads to high-amplitude photoacoustic signals of vascular structures. Thus, laser sources emitting in this spectral region are particularly suited to represent blood vessels near the surface.

Volunteers

The investigations were performed with the approval of the Ethics Committee of the Charité – Universitätsmedizin Berlin. The reference group consisted of 6 healthy volunteers (3 men and 3 women, mean age 36.2 years), who were clinically healthy at the time of the investigations and whose medical history did not show any chronic skin disease. All volunteers of the reference group exhibited skin types I–III according to the Fitzpatrick classification [30]. For the comparative study, 11 patients (4 women, 7 men; mean age 49.1 years) with known psoriasis vulgaris and an acute relapse were recruited. All volunteers of the psoriasis group exhibited skin types I–III according to the Fitzpatrick classification [30].

Study Protocol and Study Design

The first part of the study was aimed at determining the accuracy and reproducibility of the photoacoustic measurements. The related investigations were initially performed on healthy volunteers. Therefore, a skin area was marked at the volunteer's forearm and subsequently the sensor of the photoacoustic system was positioned on the marked area, the measurement was performed and the sensor was lifted. This procedure was carried out 6 times on the same skin area in order to determine the variation of the measurements. Furthermore, a total of six different skin areas on the forearm were measured. In the

second part of the study, the measurements were performed on psoriasis patients. In this case, at least 2 but not more than 3 lesional skin areas plus one adjacent non-lesional skin area were investigated.

The photoacoustic measurements were performed on standardized conditions after the subject to be tested had rested in horizontal position for at least 5 min at a room temperature between 20 and 24 °C. For the measurements, a small amount of ultrasonic gel no larger than a thumbnail was applied onto the area to be investigated. By slightly spreading the ultrasonic gel, the layer between the skin surface and the sensor should become as even as possible. With the sensor a skin surface of maximally 9.6 × 9.6 mm in size could be scanned with a step-size of 50 μm in x- and y-direction. The focused ultrasonic transducer and the resulting limited axial focusing area require the best possible parallel alignment of the sensor and the skin surface. During the measurement, which lasted 90 s, both the volunteer and the investigator should take care to minimize motion artefacts as such artefacts decisively influence the image quality.

Data Evaluation

The acquired acoustic signals were band pass filtered according to the spectral range of the transducer used in the system which minimizes the noise level. Data visualization was carried out based on the filtered data with a tailor-made software providing 2D sectional images (B-Scan) and projection images (C-Scan). The maximum amplitude projection corresponds to a tissue slice located at a defined depth parallel to the skin surface. In order to guarantee parallelism, an algorithm has been developed which detects the skin surface at each transducer position of the scanned area. Images at different depth with different slice thickness can be automatically computed.

For enhancement of the signals from the vasculature with respect to the background, a vessel enhancement filter, such as described by Frangi et al. [31], was used. Basically, the algorithm identifies cylinder-like structures by analyzing the local gradient and the Hessian matrix in any pixel of the image. The introduction of a scaling parameter allows to search for cylindrical structures of different radii. In our approach, the scaling parameter is varied and the results after filtering with different scales are compared. The scale, which maximizes the output, can then be associated to the local radius of the vessel. For the quantitative evaluation, the average vessel diameter in millimeters and the SD were determined.

Furthermore, for assessment of the vasculature ratio in the investigated region, the percentage of pixels corresponding to vessels, which correlates to the percentage of vasculature per unit volume were determined.

Statistical Evaluation

From the 6 volunteers of the healthy reference group, the arithmetic and the SD of the retrieved parameters were calculated (inter-patient variability). From the measurements of the 6 different skin areas of every volunteer of the reference group, the overall mean value, the SD, and the median value were determined (intra-patient variability).

From the group of the 11 psoriatic patients, the arithmetic mean, the SD, and the median value were calculated for the 2 or maximally 3 investigated lesional and the respective adjacent non-lesional skin areas. The skin areas of the healthy reference group and the non-lesional skin areas of the psoriatic patients were compared using the Mann-Whitney U test, whereas the Wilcoxon test was applied for comparing the lesional and the non-lesional skin areas of the psoriatic patients.

Confocal Laser Scanning Microscope

The investigations were performed using a VivaScope 1,500 Multilaser (Lucid Inc., Rochester, NY, USA). This CLSM consists of a mobile cart accommodating a laser unit that is mounted to a swivel arm. For macroscopic investigations, a camera (VivaCam) is attached to the system. The related VivaScan software enables patient data managing and filing. With the appropriate functions, skin areas can be scanned along the x–y axis (VivaBlock) and along the z-axis (VivaStack). Using the VivaBlockV function, a skin layer of maximally 8 × 8 mm in size can be scanned in one plane. The resulting single images are 500 × 500 μm in size. The VivaStack function is to be understood as an optical punch biopsy. In a specific skin area, different skin depths can be investigated along the z-axis via the software. The technical principle of CLSM is based on a laser as spot light source that is focused through a connected lens onto a specific spot in the tissue. The light reflected from the skin structures is led through a pinhole aperture and recorded by a detector. The spot light source, the tissue to be investigated, and the aperture of the pinhole are arranged confocally to each other so that only the light reflected within the tissue area in the confocal plane is imaged on the detector. The light reflected beyond this place is filtered out, thus providing a high resolution. The pinhole aperture can therefore represent only a specific image spot. In order to acquire the entire tissue, the plane to be investigated must be scanned. The individual spots of the plane under investigation are composed to form a complete image [32, 33]. The imaging procedure is based on reflectance and scattering of the individual cutaneous layers and cell structures, and depends on the refractive indices. The greater the difference between the refractive indices of the individual skin structures, the stronger the imaging contrast. Melanin and keratin, for example, exhibit a high refractive index and generate a bright contrast [34, 35]. Due to the high lateral resolution of CLSM ranging from 0.5 to 1 μm, structures can be represented even in the cellular region, although the penetration depth of CLSM into the skin is limited to between 250 and 300 μm. The axial resolution, that is, the layer thickness, amounts to approximately 3–5 μm [36, 37].

Volunteers

The investigations were performed with the approval of the Ethics Committee of the Charité – Universitätsmedizin Berlin. The reference group consisted of 6 healthy volunteers (5 women, 1 man) who were clinically healthy at the time of the investigations and whose medical history did not show any chronic skin disease. The mean age of the healthy volunteers was 37.7 years. Five volunteers of the reference group exhibited skin types I–III according to the Fitzpatrick classification [30]; one volunteer exhibited skin type V. The group of psoriatic patients consisted of 6 volunteers (3 women, 3 men; mean age 47.8 years). For the measurements, patient whose plaques were already healing and showed almost no desquamation were recruited. Five patients in the psoriasis group exhibited skin types I–III according to the Fitzpatrick classification [30] and one volunteer exhibited skin type V.

Study Protocol and Study Design

Using a CLSM, the measurements were performed on standardized conditions after the subject to be tested had rested in horizontal position for at least 5 min at a room temperature between 20 and 24 °C.

Prior to starting the investigations, the filter on the VivaScope was adjusted to reflectance and a laser wavelength of 785 nm was

Table 1. Mean value and SD from 6 repeated measurements of a marked skin area in healthy volunteers

Volunteer	Average vessel diameter, mm, mean ± SD	Vasculature per unit volume, %, mean ± SD
1	0.165±0.006	19.587±1.222
2	0.184±0.047	18.497±1.580
3	0.182±0.04	13.488±1.795
4	0.185±0.012	18.912±1.722
5	0.162±0.014	19.266±2.707
6	0.142±0.022	22.600±1.689

selected. For every volunteer, a suitable skin area on the forearm was chosen. Subsequently, 5 different regions in this skin area were captured on the stratum corneum plane by scanning along the x–y axis and via the VivaStack® function along the z-axis down to the stratum papillare. For the psoriatic patients, one non-affected and one diseased skin area, both without serious desquamation on the forearm, were investigated. Here too, 5 different regions were scanned along the z-axis down to the stratum papillare plane.

Data Evaluation

By scanning along the x–y axis, 5 single images from the selected skin area of every volunteer were captured. All papillae in a 500 × 500 μm section of the respective images at the level of the stratum papillare were counted and their maximum diameters were measured. For this purpose, a rim consisting of basal cells and melanocytes was included. The diameters were measured using the specifically developed VivaScan® software.

Statistical Evaluation

At first, the arithmetic mean and the SD of all papillary diameters in the 5 different sectional views of 500 × 500 μm per skin area of every healthy volunteer and every psoriatic patient were acquired. For comparing the papillary diameters of the healthy volunteers and the non-lesional skin areas of the psoriatic patients, the Mann-Whitney U test was applied. The Wilcoxon test was used for comparing the papillary diameters of the lesional and the non-lesional skin areas of the psoriatic patients.

Results

Photoacoustic Imaging System “SKINSPECTION”

The first part of the investigations was aimed at testing the accuracy and reproducibility of the photoacoustic measurements. Therefore, repeated measurements were performed on one marked skin area of 6 healthy volunteers, with the sensor being repositioned before each measurement. The results for the mean vascular diameter in millimeters and the percentage volume occupied by the vessels from 6 repeated measurements are represented as arithmetic mean and SD in Table 1. Despite the small

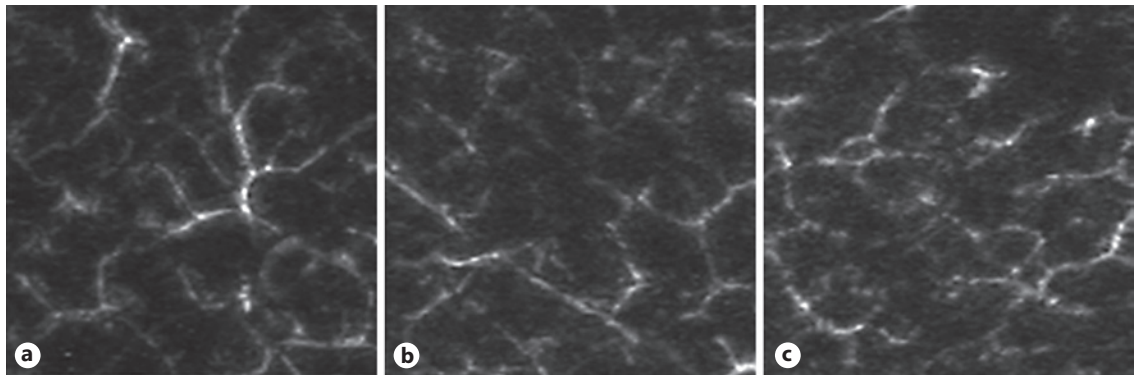


Fig. 1. a–c Each showing a 9.6×9.6 mm skin area of a healthy volunteer (**a**), non-lesional skin area of a psoriatic patient (**b**), and lesional skin area of a psoriatic patient (**c**) captured by an photoacoustic imaging system.

number of volunteers, the data indicate a high reproducibility of the measurements.

Using the photoacoustic imaging system, subcutaneous vascular networks could be visualized. A mere visual evaluation did not show a significant difference between the healthy volunteers and the lesional and non-lesional skin areas of the psoriatic patients (Fig. 1).

The quantitative comparison between the average vessel diameters in the skin of the healthy volunteers (mean value 0.229 ± 0.023 mm; median value 0.234 mm) and non-lesional skin areas of the psoriatic patients (mean value 0.225 ± 0.042 mm; median value 0.242 mm) showed no significant difference. The percentage of vasculature per unit volume in the healthy volunteers (mean value $22.395 \pm 1.501\%$; median value 23.213%) compared to that in the non-lesional areas of the psoriatic patients (mean value $24.318 \pm 4.796\%$; median value 23.078%) did not disclose a significant difference either. Comparing the average vessel diameters of lesional (mean value 0.201 ± 0.049 mm; median value 0.178 mm) and non-lesional (mean value 0.225 ± 0.042 mm; median value 0.242 mm) skin areas of psoriatic patients, no significant difference was found. Neither was a significant difference observed when comparing the measured percentage of vasculature per unit volume in the lesional (mean value $22.754 \pm 7.201\%$; median value 24.986%) and the non-lesional (mean value $24.318 \pm 4.796\%$; median value 23.078%) skin areas of the psoriatic patients.

In summary, it can be stated that neither between the healthy volunteers and the psoriatic patients nor between the lesional and the non-lesional skin areas of the psoriatic patients, significant differences were detectable in terms of the average vessel diameter and the percentage of vasculature per unit volume of the vessels of the subcutaneous plexus.

Confocal Laser Scanning Microscopy

Laser scanning microscopy was applied to determine the diameters of the dermal papillae, which were visible in the skin of the healthy volunteers as dark areas that are surrounded by a light ring consisting of basal cells and melanocytes (Fig. 2a). Based on a purely visual assessment, the dermal papillae in the lesional areas of the psoriatic patients appeared to be clearly expanded and the capillary loops inside the papillae showed an expanded vascular volume, often with visible blood flow. All in all, the capillaries seemed to be twisted. This could be recognized by sectioning the vessels several times (Fig. 2c, arrows). The non-lesional areas of the psoriatic patients did not disclose a significant expansion of the dermal papillae (Fig. 2b).

The maximum external diameters of all clearly recognizable dermal papillae in the skin of the healthy volunteers and in the lesional and non-lesional skin areas of the psoriatic patients were measured.

The overall mean value of all papillary diameters in the skin of the healthy volunteers was 0.074 ± 0.006 mm. In the non-lesional skin areas of the psoriatic patients, the overall mean value of the papillary diameters amounted to 0.079 ± 0.005 mm; in the lesional skin areas, it was 0.114 ± 0.012 mm.

No significant difference was detected in the papillary diameters in the skin of the healthy volunteers (median value 0.072 mm) compared to those of the non-lesional skin areas of psoriatic patients (median value 0.079 mm).

The results of the measurements on psoriatic patients yielded a significant difference ($p = 0.028$) between the dermal papillary diameters in the non-lesional skin areas (median value 0.079 mm) compared to those in the lesional skin areas (median value 0.116 mm).

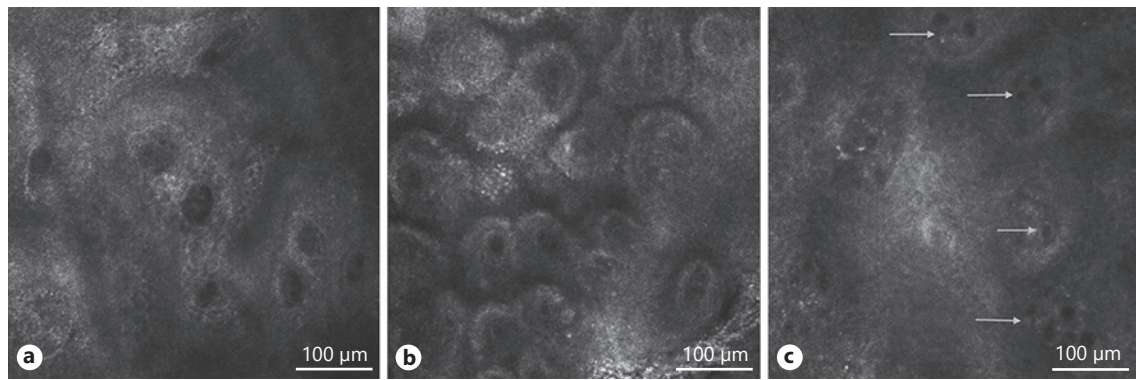


Fig. 2. a–c Confocal image of dermal papillae in a healthy volunteer (**a**), a non-lesional area (**b**), and a lesional skin area of a patient affected by psoriasis vulgaris (arrows: elongated, widened and tortuous capillary loops within the enlarged dermal papillae; **c**).

Discussion

The progress and therapy of psoriasis ought to be efficiently monitored as this disease is particularly prone to relapses, and its treatment is frequently accompanied by undesired side effects. Optimal psoriasis monitoring should facilitate an individualized therapy including modulation of a therapy in progress or starting relapse prevention, if required.

The present study was aimed at investigating photoacoustic imaging and CLSM methods for their applicability in monitoring psoriasis.

Previous investigations had already demonstrated the importance of vascular changes for the pathogenesis and the progress of psoriasis [9]. It is not precisely known if these vascular changes are related only to the loop structure or to the whole volume of the capillaries. Persistent capillary changes are supposed to promote relapses in spite of superficial healing of the skin lesion [38, 39]. In this study, the average vessel diameter and the percentage vasculature per unit volume was represented in a skin area of maximally 9.6×9.6 mm using a photoacoustic system. Investigations have demonstrated that such systems lend themselves especially for representing cutaneous vessels in vivo [20, 21]. In our study, we found that the vascular network represented with the photoacoustic imaging system applied exhibited no pathological changes. The differences in the measuring signals detected in the healthy and the pathological skin were statistically insignificant. This was not expected as the measuring methods, performed on healthy volunteers at the beginning of the investigations, had proven to be highly reproducible.

The fact that both the average vessel diameter and the percentage of vasculature per unit volume were similar in the healthy and pathological skin of the patients leads to the conclusion that the pathological changes in the vascular structure do not manifest themselves in the total volume investigated but only on the capillary loops directly underneath the skin. The resolution capacity of the photoacoustic system is insufficient to image these small subcutaneous structures. Therefore, even larger changes in this small volume are not detectable. Aguirre et al. [40] could demonstrate the effect of psoriasis on dermal microvasculature by using raster scan photoacoustic mesoscopy in an ultra-broadband mode (10–180 MHz), which achieves a higher level of detail and resolution-to-depth ratio.

In previous studies, capillary changes in psoriatic skin have been demonstrated [8, 9]. The widening of the capillaries is frequently accompanied by dilated papillae. However, the correlation between the papillary diameter and the progress of psoriasis has rarely been investigated. The investigations carried out by laser scanning microscopy in the second part of this study impressively showed significant differences in the papillary diameters of lesional (0.114 ± 0.012 mm) versus non-lesional (0.079 ± 0.005 mm) skin areas of psoriatic patients. No difference could be found between the papillary diameters in the skin of healthy patients compared to those in non-lesional skin of psoriatic patients. Ardigo et al. [41] investigated the applicability of confocal light microscopy for therapeutic psoriasis monitoring. In this case, dermal papillae of >100 µm in diameter were defined as being widened. A significant reduction of the papillary diameters and the widened vessels within the papillae subsequent of 8 weeks of therapy with a tumor necrosis factor- α antibody could be shown. In a study, Archid

et al. [12] could also demonstrate a distinct widening of the papillary diameters ($146.46 \pm 28.52 \mu\text{m}$) in psoriatic skin as well as a significant difference to healthy skin ($69.48 \pm 17.16 \mu\text{m}$). The papillary diameters in psoriatic skin measured in that study contradicts our results ($0.114 \pm 0.012 \text{ mm}$). This discrepancy could be due to the fact that our psoriatic were examined during therapy, whereas Archid et al. [42] included only patients into their study who had not received any anti-psoriatic therapy in the 2 months prior to the study. Interestingly, a further investigation conducted by Archid et al. [42] on 11 patients showed that, in terms of the percentage reduction of the Psoriasis Area Severity Index value, a clinical improvement under Goeckerman therapy correlated with a normalization of the papillary structure rather than of the capillaries [42]. Another study performed by Ardigo et al. [43] showed separate tendencies in the microscopic changes during the administration of 2 local therapeutics of different effects. These results suggest that laser scanning microscopy could be a suitable method for psoriasis monitoring. However, there are also considerable restrictions for the application of laser scanning microscopy to psoriatic skin investigations. In another study, Ardigo et al. [44] could find a strong correlation between CLSM and histology in terms of psoriasis assessment. However, a high degree of hyperkeratosis, parakeratosis, acanthosis, and spongiosis can lead to a reduced penetration of light into the tissue, thus impeding the assessment of the dermal papillae and the dermo-epidermal junction [44]. Here as well, a distinct widening of the papillary diameters (median value $151 \mu\text{m}$) compared to the control group (median value $<80 \mu\text{m}$) in psoriatic skin could be determined. In this case, the papillary diameters in psoriatic skin, which conflicted with our results ($0.114 \pm 0.012 \text{ mm}$) can also be explained by the fact that Ardigo et al. [44] only included psoriatic patients into their study, who had not received any systemic or topical therapy within the previous 4 months. The assessment of the dermal papillae can also be impeded by low melanin concentrations and, consequently, low contrast CLSM images [34, 45]. Lagarrigue et al. [46] could show in a study on 111 volunteers that the papillary contrast as measured in the dermo-epithelial junction seems to be a reliable marker for skin pigmentation and clearly correlates with the skin types according to the Fitzpatrick classification [30]. Consequently, an assessment of the dermal papillae in patients of skin types I and II according to the Fitzpatrick classification [30] is impeded [45, 46]. In addition, a lacking papillary ring in psoriatic skin may limit the assessment of the dermal papillae. In their study involving 36 psoriatic patients, Ardigo et al. [44] could show that in 86% of the psoriatic lesions, the dermal papillae were not surrounded by a bright papillary ring consisting of basal keratinocytes and melanocytes. This ring was only recognizable as a shadowy structure [44]. This may be due to an inhibition of the melanin synthesis or the increasing apoptosis of melanocytes, which is triggered by the tumor necrosis factor- α [44, 47]. Further investigations are required to elucidate these changes in psoriatic skin.

In summary, the investigations have shown that the pathological changes in the vascular structures of psoriatic patients manifest themselves predominantly in the capillary loops but not in the deeper blood vessels. As the resolution of the photoacoustic system applied was not high enough to represent the changes in the structure of the capillary loops, the performed photoacoustic measurements are unsuitable for the described investigations. To make it suitable, the frequency of the ultrasonic transducer would have to be increased, so that a higher resolution can be achieved [40]. Consequently, laser scanning microscopy remains the method of choice for the detection of pathological changes in psoriatic skin. Laser scanning microscopy is already established in dermatology, and the papillary diameter is a parameter relatively easy to measure. The determination of the papillary diameter seems to be suitable for monitoring the clinical course in psoriasis.

Statement of Ethics

Approval of the study was obtained from the Ethic Commission of the Charité - reference EA1/138/12.

Disclosure Statement

The authors declare no conflict of interest.

References

- 1 Michalek IM, Loring B, John SM: A systematic review of worldwide epidemiology of psoriasis. *J Eur Acad Dermatol Venereol* 2017;31: 205–212.
- 2 Farkas A, Kemeny L: Alcohol, liver, systemic inflammation and skin: a focus on patients with psoriasis. *Skin Pharmacol Physiol* 2013; 26:119–126.
- 3 Tohid H, Aleem D, Jackson C: Major depression and psoriasis: a psychodermatological phenomenon. *Skin Pharmacol Physiol* 2016; 29:220–230.
- 4 Berger K, Ehlken B, Kugland B, Augustin M: Cost-of-illness in patients with moderate and severe chronic psoriasis vulgaris in Germany. *J Dtsch Dermatol Ges* 2005;3:511–518.

- 5 Rapp SR, Feldman SR, Exum ML, Fleischer AB Jr, Reboussin DM: Psoriasis causes as much disability as other major medical diseases. *J Am Acad Dermatol* 1999;41:401–407.
- 6 Fitch E, Harper E, Skorcheva I, Kurtz SE, Blauvelt A: Pathophysiology of psoriasis: recent advances on IL-23 and Th17 cytokines. *Curr Rheumatol Rep* 2007;9:461–467.
- 7 Zheng Y, Danilenko DM, Valdez P, Kasman I, Eastham-Anderson J, Wu J, Ouyang W: Interleukin-22, a T(H)17 cytokine, mediates IL-23-induced dermal inflammation and acanthosis. *Nature* 2007;445:648–651.
- 8 Braverman IM, Sibley J: Role of the microcirculation in the treatment and pathogenesis of psoriasis. *J Invest Dermatol* 1982;78:12–17.
- 9 Braverman IM, Yen A: Ultrastructure of the capillary loops in the dermal papillae of psoriasis. *J Invest Dermatol* 1977;68:53–60.
- 10 Mrowietz U, Kragballe K, Reich K, Spuls P, Griffiths CE, Nast A, Franke J, Antoniou C, Arenberger P, Balieva F, Bylaite M, Correia O, Dauden E, Gisondi P, Iversen L, Kemeny L, Lahfa M, Nijsten T, Rantanen T, Reich A, Rosenbach T, Segaert S, Smith C, Talme T, Volc-Platzer B, Yawalkar N: Definition of treatment goals for moderate to severe psoriasis: a European consensus. *Arch Dermatol Res* 2011;303:1–10.
- 11 Lebwohl M: A clinician's paradigm in the treatment of psoriasis. *J Am Acad Dermatol* 2005;53:S59–S69.
- 12 Archid R, Patzelt A, Lange-Asschenfeldt B, Ahmad SS, Ulrich M, Stockfleth E, Philipp S, Sterry W, Lademann J: Confocal laser-scanning microscopy of capillaries in normal and psoriatic skin. *J Biomed Opt* 2012;17:101511.
- 13 Wolberink EA, van Erp PE, de Boer-van Huijzen RT, van de Kerkhof PC, Gerritsen MJ: Reflectance confocal microscopy: an effective tool for monitoring ultraviolet B phototherapy in psoriasis. *Br J Dermatol* 2012;167:396–403.
- 14 Su JL, Wang B, Wilson KE, Bayer CL, Chen YS, Kim S, Homan KA, Emelianov SY: Advances in clinical and biomedical applications of photoacoustic imaging. *Expert Opin Med Diagn* 2010;4:497–510.
- 15 Wang S, Lin J, Wang T, Chen X, Huang P: Recent advances in photoacoustic imaging for deep-tissue biomedical applications. *Theranostics* 2016;6:2394–2413.
- 16 Kruger RA, Lam RB, Reinecke DR, Del Rio SP, Doyle RP: Photoacoustic angiography of the breast. *Med Phys* 2010;37:6096–6100.
- 17 Manohar S, Vaartjes SE, van Hespden JC, Klaase JM, van den Engh FM, Steenbergen W, van Leeuwen TG: Initial results of in vivo non-invasive cancer imaging in the human breast using near-infrared photoacoustics. *Opt Express* 2007;15:12277–12285.
- 18 Oh JT, Li ML, Zhang HF, Maslov K, Stoica G, Wang LV: Three-dimensional imaging of skin melanoma in vivo by dual-wavelength photoacoustic microscopy. *J Biomed Opt* 2006;11:34032.
- 19 Zhang HF, Maslov K, Stoica G, Wang LV: Imaging acute thermal burns by photoacoustic microscopy. *J Biomed Opt* 2006;11:054033.
- 20 Favazza CP, Cornelius LA, Wang LV: In vivo functional photoacoustic microscopy of cutaneous microvasculature in human skin. *J Biomed Opt* 2011;16:026004.
- 21 Favazza CP, Jassim O, Cornelius LA, Wang LV: In vivo photoacoustic microscopy of human cutaneous microvasculature and a nevus. *J Biomed Opt* 2011;16:016015.
- 22 Nuster R, Schmitner N, Wurzingger G, Gratt S, Salvenmoser W, Meyer D, Paltauf G: Hybrid photoacoustic and ultrasound section imaging with optical ultrasound detection. *J Biophotonics* 2013;6:549–559.
- 23 Paltauf G, Schmidt-Kloiber H: [Optoacoustic spectroscopy and imaging]. *Z Med Phys* 2002;12:35–42.
- 24 Zackrisson S, van de Ven S, Gambhir SS: Light in and sound out: emerging translational strategies for photoacoustic imaging. *Cancer Res* 2014;74:979–1004.
- 25 Yao J, Wang LV: Photoacoustic tomography: fundamentals, advances and prospects. *Contrast Media Mol Imaging* 2011;6:332–345.
- 26 Beard P: Biomedical photoacoustic imaging. *Interface Focus* 2011;1:602–631.
- 27 Mallidi S, Luke GP, Emelianov S: Photoacoustic imaging in cancer detection, diagnosis, and treatment guidance. *Trends Biotechnol* 2011;29:213–221.
- 28 Valluru KS, Chinni BK, Rao NA: Photoacoustic imaging: opening new frontiers in medical imaging. *J Clin Imaging Sci* 2011;1:24.
- 29 Jose J, Manohar S, Kolkman RG, Steenbergen W, van Leeuwen TG: Imaging of tumor vasculature using Twente photoacoustic systems. *J Biophotonics* 2009;2:701–717.
- 30 Fitzpatrick TB: The validity and practicality of sun-reactive skin types I through VI. *Arch Dermatol* 1988;124:869–871.
- 31 Frangi AF, Niessen WJ, Vincken KL, Viergever MA: Multiscale vessel enhancement filtering. In *Medical Image Computing and Computer-Assisted Intervention, MICCAI 98, Lecture Notes in Computer Science*, vol 1496, Springer, Berlin, 130–137.
- 32 Nwaneshiudu A, Kuschal C, Sakamoto FH, Anderson RR, Schwarzenberger K, Young RC: Introduction to confocal microscopy. *J Invest Dermatol* 2012;132:e3.
- 33 Ulrich M, Lange-Asschenfeldt S: In vivo confocal microscopy in dermatology: from research to clinical application. *J Biomed Opt* 2013;18:061212.
- 34 Rajadhyaksha M, Grossman M, Esterowitz D, Webb RH, Anderson RR: In vivo confocal scanning laser microscopy of human skin: melanin provides strong contrast. *J Invest Dermatol* 1995;104:946–952.
- 35 Meyer LE, Lademann J: Application of laser spectroscopic methods for in vivo diagnostics in dermatology. *Laser Physics Letters* 2007;4:754.
- 36 Astner S, Ulrich M: [Confocal laser scanning microscopy]. *Hautarzt* 2010;61:421–428.
- 37 Rajadhyaksha M, Gonzalez S, Zavislan JM, Anderson RR, Webb RH: In vivo confocal scanning laser microscopy of human skin II: advances in instrumentation and comparison with histology. *J Invest Dermatol* 1999;113:293–303.
- 38 Braverman IM, Sibley J: The response of psoriatic epidermis and microvessels to treatment with topical steroids and oral methotrexate. *J Invest Dermatol* 1985;85:584–586.
- 39 Musumeci ML, Lacarrubba F, Fusto CM, Micali G: Combined clinical, capillaroscopic and ultrasound evaluation during treatment of plaque psoriasis with oral cyclosporine. *Int J Immunopathol Pharmacol* 2013;26:1027–1033.
- 40 Aguirre J, Schwarz M, Garzorz N, Omar M, Buehler A, Eyerich K, Ntziachristos V: Precision assessment of label-free psoriasis biomarkers with ultra-broadband optoacoustic mesoscopy. *Nat Biomed Eng* 2017;1:0068.
- 41 Ardigo M, Agozzino M, Longo C, Lallas A, Di Lernia V, Fabiano A, Conti A, Sperduti I, Argenziano G, Berardesca E, Pellacani G: Reflectance confocal microscopy for plaque psoriasis therapeutic follow-up during an anti-TNF- α monoclonal antibody: an observational multicenter study. *J Eur Acad Dermatol Venereol* 2015;29:2363–2368.
- 42 Archid R, Duerr HP, Patzelt A, Philipp S, Rowert-Huber HJ, Ulrich M, Meinke MC, Knorr F, Lademann J: Relationship between histological and clinical course of psoriasis: a pilot investigation by reflectance confocal microscopy during goeckerman treatment. *Skin Pharmacol Physiol* 2016;29:47–54.
- 43 Ardigo M, Agozzino M, Longo C, Conti A, Di Lernia V, Berardesca E, Pellacani G: Psoriasis plaque test with confocal microscopy: evaluation of different microscopic response pathways in NSAID and steroid treated lesions. *Skin Res Technol* 2013;19:417–423.
- 44 Ardigo M, Cota C, Berardesca E, Gonzalez S: Concordance between in vivo reflectance confocal microscopy and histology in the evaluation of plaque psoriasis. *J Eur Acad Dermatol Venereol* 2009;23:660–667.
- 45 Robertson K, Rees JL: Variation in epidermal morphology in human skin at different body sites as measured by reflectance confocal microscopy. *Acta Derm Venereol* 2010;90:368–373.
- 46 Lagarrigue SG, George J, Questel E, Lauze C, Meyer N, Lagarde JM, Simon M, Schmitt AM, Serre G, Paul C: In vivo quantification of epidermis pigmentation and dermis papilla density with reflectance confocal microscopy: variations with age and skin phototype. *Exp Dermatol* 2012;21:281–286.
- 47 Martinez-Esparza M, Jimenez-Cervantes C, Solano F, Lozano JA, Garcia-Borrón JC: Mechanisms of melanogenesis inhibition by tumor necrosis factor- α in B16/F10 mouse melanoma cells. *Eur J Biochem* 1998;255:139–146.